

O-2p holes in tetravalent oxides of Ce and Pr and the Fehrenbacher-Rice hybrid in PrBa₂Cu₃O_{7- δ}

Z. Hu, R. Meier, C. Schüßler-Langeheine, E. Weschke, and G. Kaindl

Institut für Experimentalphysik, Freie Universität Berlin, Arnimallee 14, D-14195 Berlin-Dahlem, Germany

I. Felner

Racah Institute of Physics, The Hebrew University of Jerusalem, Jerusalem 91904, Israel

M. Merz, N. Nücker, and S. Schuppler

INFP, Forschungszentrum Karlsruhe, P.O. Box 3640, D-76021 Karlsruhe, Germany

A. Erb

Département de Physique de la Matière Condensée, Université de Genève, 24, quai Ernest-Ansermet, CH-1211 Genève-4, Switzerland

(Received 26 February 1999)

We report on an x-ray absorption near-edge structure (XANES) study of O-2p holes induced by Ln-4f/O-2p covalence in LnO₂ (Ln=Ce,Pr) and BaLnO₃ (Ln=Ce,Pr,Tb). The pre-edge peak in the O-1s XANES spectra, associated with O-2p holes, shifts to lower energy from Ce to Pr, in agreement with theoretical expectation, and its intensity scales with the strength of the 4f/2p covalence. In Pr(IV) oxides, the pre-edge peak is at the energy of the ‘‘Fehrenbacher-Rice’’ state in PrBa₂Cu₃O_{7- δ} , supporting the view that the suppression of superconductivity in PrBa₂Cu₃O_{7- δ} is due to Pr-4f/O-2p hybridization. [S0163-1829(99)11619-9]

In the last decade, the multiple peaks in the x-ray absorption near-edge structure (XANES) and core-level photoemission (PE) spectra of tetravalent lanthanide compounds, like LnO₂ (Ln=Ce,Pr,Tb), LnF₄ (Ln=Ce,Tb), and M₃LnF₇ (M=Cs,Rb; Ln=Ce,Pr,Nd,Tb,Dy) have evoked a series of theoretical and experimental efforts concerning 4f valence and covalence.¹⁻⁴ The observed spectral features can be well interpreted by Ln-4f/ligand-2p covalence within the framework of the Anderson impurity model. In this model, the ground-state wave function is given by $\phi_g = \alpha_0|4f^n\rangle + \beta_0|4f^{n+1}\underline{L}\rangle$, where $n=0, 1, 2, 7, 8$ refers to Ce, Pr, Nd, Tb, Dy, respectively, and \underline{L} stands for a hole in the ligand-2p orbitals (here, mixing with $4f^{n+2}\underline{L}^2$ configurations is neglected). These results on tetravalent lanthanide compounds receive attention in connection with the suppression of superconductivity in YBa₂Cu₃O_{7- δ} , when Y is substituted by Pr, with the orthorhombic structure being preserved. While substitution by Ce also depresses T_c , substitution by the heavy lanthanide element Tb, with only a weak Tb-4f/O-2p hybridization, hardly affects T_c .⁵

The present work has two main objectives. (i) To gain direct information on the ligand holes induced by Ln-4f/O-2p covalence in these tetravalent oxides in order to set up a reference for a better understanding of the electronic structure of related more complex materials, such as high- T_c superconductors. (ii) To compare the electronic structure of PrO₂ and PrBa₂Cu₃O_{7- δ} near E_F . Concerning (i), we note that for low- Z elements, the creation of a core hole in the XANES process has only little effect on the unoccupied states just above E_F ,⁶ allowing us to analyze in a quite direct way via O-1s XANES the ligand holes induced by Ln-4f/O-2p covalence in the ground state. This method has been applied previously to high- T_c materials,⁷⁻⁹ but not to

tetravalent LnO₂, where information on O-2p holes has only been obtained in a rather indirect way from Ln core-level spectra.^{1,3} With regard to (ii), the LnO₂ and BaLnO₃ oxides—due to their simple crystal structures—are ideally suited for a comparison of the Ln-4f/O-2p hybridization in these compounds with that in PrBa₂Cu₃O₇. We shall thus present O-1s XANES spectra of CeO₂ and PrO₂, with cubic local symmetry around the Ln ion, and of BaCeO₃, BaPrO₃, and BaTbO₃, with octahedral local symmetry around Ln. We compare the results with O-1s XANES spectra obtained from single-crystalline PrBa₂Cu₃O_{7- δ} , where the Ln-4f/O-2p bonding is expected to be similar to PrO₂ on the basis of the same symmetry.

The XANES measurements on CeO₂, PrO₂, BaCeO₃, BaPrO₃, and BaTbO₃ were performed in the total-electron-yield (TEY) mode at the SX700/II beamline operated by the Freie Universität Berlin at the Berliner Elektronenspeicherung für Synchrotronstrahlung (BESSY). The experimental resolution was 300 meV [full width at half maximum (FWHM)] at a photon energy of 530 eV. The tetravalent Ln oxide samples were in the form of polycrystalline pressed pellets (12 mm diameter, 3 mm thick). They were transferred from a clean Ar atmosphere to the experimental chamber with a base pressure of 1×10^{-10} mbar, and scraped with a diamond file prior to the measurements. The data were normalized to TEY spectra of Au in order to account for variations of the incident photon flux as a function of photon energy. They were also normalized at 50 eV above the absorption threshold, where the density of states has almost free-electron-like character. The purities of the samples were checked by Ln- $M_{4,5}$ XANES, which revealed pure Ln(IV) states in BaLnO₃ and CeO₂. In the case of PrO₂, about 9% Pr(III) impurities were found, in agreement with the fact that

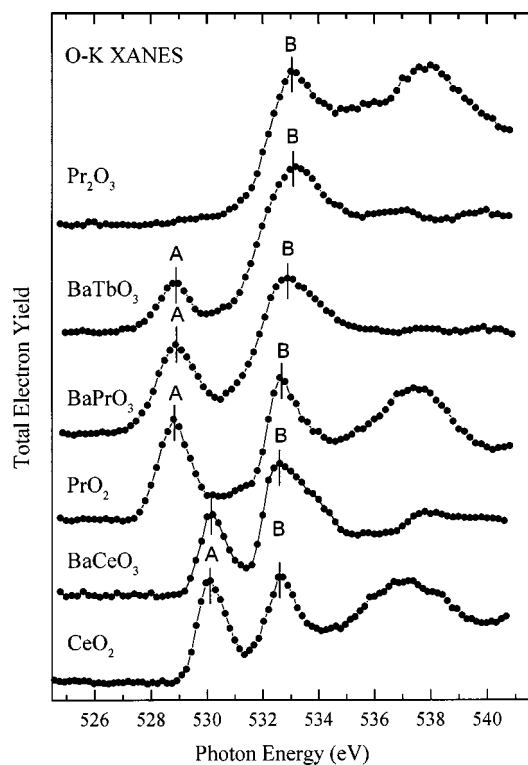


FIG. 1. O-1s XANES spectra of the tetraivalent Ln oxides CeO_2 , PrO_2 , BaCeO_3 , BaPrO_3 , BaTbO_3 , and of Pr_2O_3 for comparison; the spectra were taken in the total-electron-yield mode.

stoichiometric PrO_2 is known to be only stable under oxygen pressure.¹⁰ The polarization-dependent O-1s XANES spectra of a detwinned single crystal of $\text{PrBa}_2\text{Cu}_3\text{O}_{7-\delta}$ ($\delta \approx 0.09$) were recorded at the National Synchrotron-Radiation Light Source (NSLS), Brookhaven National Laboratory, employing the Naval Research Laboratory beamline O4B. In this case, the rather bulk-sensitive fluorescence-yield (FY) mode was employed, using a seven-element ultra-low-energy Ge detector (with a typical sampling depth of $\approx 1000 \text{ \AA}$ as compared to $\approx 30 \text{ \AA}$ in the TEY mode).^{7,8,11} The resolution at this beamline was 210 meV (FWHM) at a photon energy of 530 eV. I_0 normalization (at $\approx 70 \text{ eV}$ above threshold) and self-absorption correction were performed in the usual way, as described in detail in Ref. 11. In the case of the O-1s spectra, FY is a good measure of the absorption, since multiplet splitting can be neglected.¹²

Figure 1 displays the O-1s XANES spectra of CeO_2 , PrO_2 , BaCeO_3 , BaPrO_3 , BaTbO_3 , and of Pr_2O_3 for comparison. The spectral features observed for the Ln_2O_3 compounds are all very similar to the spectrum shown for Pr_2O_3 , with a strong peak B at $\approx 533 \text{ eV}$ superimposed on the edge jump, and a broad structure centered at $\approx 538 \text{ eV}$. Peak B and the structure at $\approx 538 \text{ eV}$ are assigned to Ln-5d and Ln-6p states, respectively, while the edge jump corresponds to transitions to empty continuum states. In the spectra of the tetraivalent Pr compounds, shown in Fig. 1, peak B is also assigned to Pr-5d states. The pre-edge regions are particularly interesting in the spectra of the tetraivalent oxides, since these contain a pre-edge peak A located $\approx 4.2 \text{ eV}$ below peak B; this reveals unoccupied states below the Pr-5d derived states. Such a pre-edge peak was also observed in the XANES spectrum of Pr_6O_{11} with about the same energy dif-

ference to the main peak as in the spectrum of Pr_2O_3 . However, it was only poorly resolved due to insufficient experimental resolution, and the relative intensity of the pre-edge peak was found to be weaker than in PrO_2 , in accordance with about 30% Pr(III) in this mixed-valent oxide.⁹ It should be noted that the given assignments of 4f and 5d character to features A and B, respectively, are consistent with the results of bremsstrahlung isochromat spectroscopy¹³ (BIS) and optical reflectivity measurements.¹⁴

The pre-edge peak A reflects transitions of a 1s core electron to 2p-hole states in the narrow 4f-dominated bands resulting from strong Pr-4f/O-2p hybridization in the ground states of tetravalent Pr compounds. This is consistent with the view that covalence increases with increasing valence of the metal ion.¹⁵ In the case of tetravalent Ln fluorides, the pre-edge peak is shifted further to lower energies by $\approx 7 \text{ eV}$ with respect to LnF_3 , far below the edge jump.⁴ If we neglect the change of the hole distribution induced by the core hole, the relative intensity of the pre-edge peak is proportional to $|\beta_0|^2$ (see Introduction), since in XANES only intra-atomic transition matrix elements have nonzero magnitude. We also note that, in spite of the different crystal structures of PrO_2 and BaPrO_3 , the spectral profiles and energy positions of the pre-edge peaks are quite similar for the two oxides. On the other hand, differences are observed in the energy region of peak B and above, which result from different Ln-5d and Ln-6sp band structures due to the different crystal structures.

A pre-edge peak A is also observed for BaTbO_3 , however, with a rather low spectral weight (analogous to the F-1s XANES spectra of tetravalent Ln fluorides⁴). This reflects a weak Tb-4f/O-2p hybridization in this heavy Ln oxide due to the small 4f radius of Tb. The XANES profiles of CeO_2 and BaCeO_3 are quite similar to those of PrO_2 and BaPrO_3 , which is not unexpected since the crystal structures of LnO_2 and BaLnO_3 are the same and the Ln-4f/O-2p hybridizations ought to be of comparable strengths. The only obvious difference is a shift of the pre-edge peak A to lower energies by $\approx 1.3 \text{ eV}$, similar to the situation found for the tetravalent Ln fluorides.⁴ Such a shift has also been observed from Cu(II)/Cu(III) to Ni(II)/Ni(III) in a previous study, where a systematic shift of the pre-edge peak to lower energies was found when the ionization energy of the metal ion in the same oxidation state increases.^{15,16} Along this line, we arrive at a consistent picture by noting that the fourth ionization potential of Pr(IV) is $E_{i,4} = 38.98 \text{ eV}$, while it is 36.76 eV for Ce(IV).¹⁷

The intensities of the pre-edge peak A for the BaLnO_3 series scale approximately as 1:2.2:2.6 in the sequence Tb:Ce:Pr. To arrive at an estimate for the absolute hole counts, we recall that for CeO_2 a value of 0.48 has been deduced from Ln core-level spectra.^{1,3,18} This value appears quite reliable since the Ce(IV) state, with a formal 4f⁰ configuration, is highly stable, while for other Ln(IV) oxides, like PrO_2 and TbO_2 , substantial Ln(III) impurities are always present, leading to overestimates of the hole counts.^{3,18} Therefore, we deem it appropriate to scale the BaLnO_3 series by setting the intensity of the pre-edge peak in BaCeO_3 equal to 0.48 holes, which leads to hole counts of 0.57 for BaPrO_3 and 0.22 for BaTbO_3 .

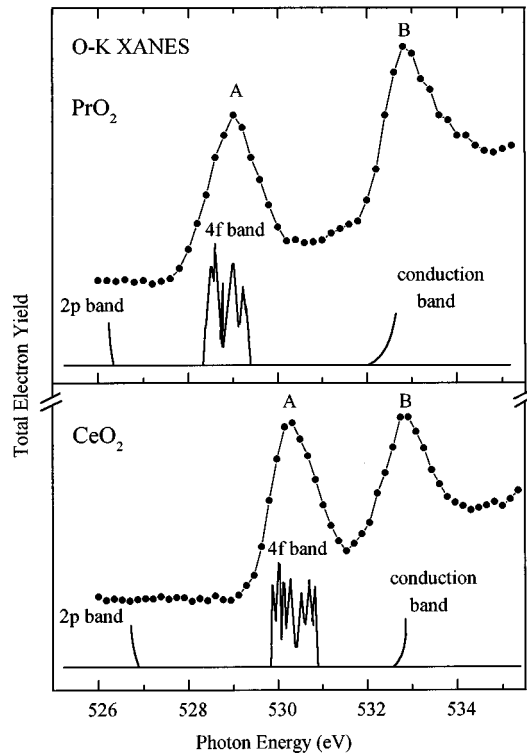


FIG. 2. O-1s XANES spectra of the tetravalent Ln oxides CeO_2 (bottom panel) and PrO_2 (top panel), and calculated densities of states from Ref. 10 for comparison; the spectra were taken in the total-electron-yield mode.

We now turn to a comparison of the O-1s XANES spectra of LnO_2 ($\text{Ln}=\text{Ce,Pr}$) with the results of self-consistent-field (SCF) band-structure calculations, neglecting possible O-1s core-hole effects. The results are presented in Fig. 2, where in addition to the O-1s XANES spectrum of PrO_2 (top panel) and CeO_2 (bottom panel) the partial densities of states from the SCF band-structure calculations of Koelling, Boring, and Wood¹⁰ are displayed (note that the detailed 2p bands below E_F are not reproduced in Fig. 2). We note that the calculated bands agree very well with the observed spectral structures, supporting the given assignments. Moreover, the energy separations between the 4f and 5d bands are well reproduced for each compound, as are the differences between the two compounds. In addition, the good agreement shows that the O-1s core level has only minor effects on the unoccupied states in the two compounds. On the basis of Fig. 2 one can also readily understand the metallic and insulating properties of PrO_2 and CeO_2 , respectively. Thus, both the Anderson impurity model and the band-structure calculations are able to describe the electronic structure of the LnO_2 compounds. It is obvious from this discussion that the pre-edge peak A is not of the same origin as structure B (at ≈ 533 eV), in contrast to what had been claimed in Ref. 9; instead it is due to Pr-4f/O-2p hybridization. With this understanding of the Pr-4f/O-2p hybridization in PrO_2 and BaPrO_3 , we now turn to the more complex material $\text{PrBa}_2\text{Cu}_3\text{O}_{7-\delta}$.

Figure 3 compares the O-1s XANES spectrum of PrO_2 (top spectrum) with polarization-dependent O-1s XANES spectra of detwinned, single-crystalline $\text{PrBa}_2\text{Cu}_3\text{O}_{7-\delta}$ (bot-

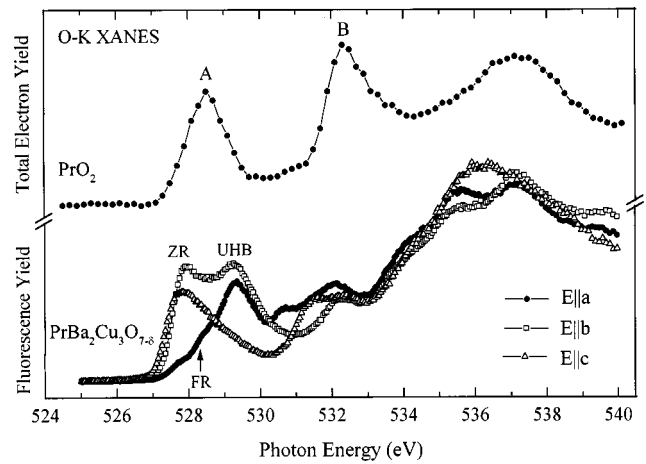


FIG. 3. Comparison of the O-1s XANES spectrum of PrO_2 measured in the total-electron-yield mode with those of $\text{PrBa}_2\text{Cu}_3\text{O}_{7-\delta}$ taken in the fluorescence-yield mode for $\mathbf{E}\parallel\mathbf{a}$ (filled circles), $\mathbf{E}\parallel\mathbf{b}$ (open squares), and $\mathbf{E}\parallel\mathbf{c}$ (open triangles).

tom spectra). The suppression of T_c upon replacing Y by Pr has been attributed to one of the following mechanisms (for a more complete discussion of the various other explanations proposed and their respective support or refutation by experiments, see Ref. 19).

(i) The magnetic moment of the Pr(IV) ion, mediated to the CuO_2 planes by some Pr-4f admixture to the O-2p orbitals, leads to pair breaking.¹⁹

(ii) Pr-4f/O-2p $_{\pi}$ hybridization in the so-called ‘‘Fehrenbacher-Rice’’ (FR) state²⁰ competes energetically with the ‘‘usual’’ planar Cu-3d/O-2p $_{\sigma}$ hybridization in the Zhang-Rice (ZR) state.²¹ The latter is generally believed to carry superconductivity in high- T_c materials. In the FR model, a slight energy advantage is postulated in favor of the FR state, thus leaving effectively no carriers in the ZR state for superconductivity. Clearly, for FR states to exist, some fraction of the Pr ions in $\text{PrBa}_2\text{Cu}_3\text{O}_{7-\delta}$ has to be in the Pr(IV) state.

$\text{PrBa}_2\text{Cu}_3\text{O}_7$ had been studied previously by XANES at the Pr- $L_{\text{II,III}}$ thresholds, with the spectral profile of the Pr(IV) component found to be rather similar to that of PrO_2 .²² This agreement is due to the fact that the local symmetries of the Pr ions in these two compounds are quite similar, considering the fact that the final state in the XANES process, Pr-5d, is rather sensitive to the local environment. Roughly 10% Pr(IV) spectral weight had been estimated in that work. As shown in Fig. 3, the perovskite-related material $\text{PrBa}_2\text{Cu}_3\text{O}_{7-\delta}$ exhibits a rich XANES structure close to E_F , due to the large number of inequivalent O sites. This makes it necessary to study detwinned single crystals, in order to be able to distinguish between contributions from the various sites. Details of the procedure can be found in Ref. 19, and the assignment given below follows closely the arguments presented there.

The first absorption feature at ≈ 527.8 eV in the spectra with light polarization \mathbf{E} oriented parallel to the crystallographic \mathbf{b} and \mathbf{c} axes corresponds to holes in the O(1) chain site and the O(4) apical site, respectively, and will not be considered in the following. The $\mathbf{E}\parallel\mathbf{a}$ spectrum exhibits a prominent peak at 529.3 eV, which was shown previously to

correspond to the upper Hubbard band.¹⁹ On the leading edge of this peak, a shoulder is observed (marked by a vertical arrow), which is close to the energy of the ZR state in $\text{PrBa}_2\text{Cu}_3\text{O}_7$. However, as shown in previous studies of $\text{Pr}_{0.8}\text{Y}_{0.2}\text{Ba}_2\text{Cu}_3\text{O}_{7-\delta}$, this shoulder cannot be the result of Cu/O hybridization (as the ZR state), since in that case the transfer of spectral weight would lower the upper Hubbard band considerably. Instead, it is a strong indication of O orbitals in the Cu-O planes that are hybridized with Pr, but not with Cu, i.e., forming FR states. Note that the pre-edge peak A in the spectrum of PrO_2 is located very close to the energy of the “FR shoulder,” an observation that lends further support to an interpretation of this shoulder as due to Pr-4*f*/O-2*p* hybridization. The fact that according to the FR model, 50% of the Pr ions ought to be tetravalent, however, should not be confused with a charge transfer of this magnitude. Instead, Fehrenbacher and Rice arrive at about 0.2 holes transferred on the average to the Pr site, which corresponds approximately to the amount of holes “missing” from the O sites in a quantitative analysis of the $\text{Pr}_{0.8}\text{Y}_{0.2}\text{Ba}_2\text{Cu}_3\text{O}_{7-\delta}$ spectra.¹⁹ This explains the relatively small intensity of the FR shoulder in Fig. 3.

The ligand holes induced by Ln-4*f*/O-2*p* hybridization in the Ln(IV) oxides, CeO_2 , PrO_2 , BaCeO_3 , BaPrO_3 , and BaTbO_3 , were directly observed in O-1*s* XANES spectra in the form of characteristic pre-edge peaks. This observation confirms the proposal of Ln-4*f*/O-2*p* covalence suggested in previous studies by Ln core-level spectroscopy. The energy positions of the pre-edge peaks vary with the Ln element, with the trend being in agreement with the results of SCF band-structure calculations. The weak intensity of the pre-edge peak observed for BaTbO_3 is explained by a weak Tb-4*f*/O-2*p* covalence in this compound. Furthermore, the spectral similarities between the O-1*s* XANES spectra of PrO_2 and $\text{PrBa}_2\text{Cu}_3\text{O}_{7-\delta}$ give support to the view that the suppression of superconductivity in the latter compound is caused by Fehrenbacher-Rice Pr-4*f*/O-2*p* hybridization, which removes holes necessary for superconductivity from the planar Cu-3*d*/O-2*p* hybridized orbitals.

This work was supported by the Deutsche Forschungsgemeinschaft, Project No. Ka 564/7-2, and the Bundesminister für Bildung, Wissenschaft, Forschung und Technologie, Project No. 13 N-6601/0.

¹A. Kotani *et al.*, Solid State Commun. **53**, 805 (1985).

²G. Kaindl *et al.*, Phys. Rev. Lett. **58**, 606 (1987).

³A. Bianconi *et al.*, Phys. Rev. B **35**, 806 (1987).

⁴Z. Hu, G. Kaindl, and B. G. Müller, J. Alloys Compd. **246**, 177 (1997).

⁵C. R. Fincher, Jr. and Graciela B. Blanchet, Phys. Rev. Lett. **67**, 2902 (1992).

⁶F. M. F. de Groot *et al.*, Phys. Rev. B **40**, 5715 (1989).

⁷J. Fink *et al.*, Phys. Rev. B **42**, R4823 (1990).

⁸D. D. Sarma *et al.*, Solid State Commun. **77**, 377 (1991).

⁹A. Hartmann and G. J. Russell, Solid State Commun. **95**, 791 (1995).

¹⁰D. D. Koelling, A. M. Boring, and J. M. Wood, Solid State Commun. **4**, 227 (1983).

¹¹E. Pellegrin *et al.*, Phys. Rev. B **47**, 3354 (1993).

¹²F. M. F. de Groot *et al.*, Solid State Commun. **92**, 991 (1994).

¹³E. Wuilloud *et al.*, Phys. Rev. Lett. **53**, 202 (1984).

¹⁴F. Marabelli and P. Wachter, Phys. Rev. B **36**, 1238 (1987).

¹⁵Z. Hu *et al.*, Chem. Phys. **232**, 63 (1998).

¹⁶C. Sugiura and T. Suzuki, J. Chem. Phys. **75**, 4357 (1981).

¹⁷W. C. Martin, R. Zalubas, and L. Hagan, in *Atomic Energy Levels—The Rare-Earth Elements*, Natl. Bur. Stand. (U.S.) Ref. Data Ser. No. 60, edited by W. C. Martin, Romuald Zalubas, and Lucy Hagan (U.S. GPO, Washington, DC, 1978).

¹⁸T. Ikeda *et al.*, J. Phys. Soc. Jpn. **59**, 622 (1990).

¹⁹M. Merz *et al.*, Phys. Rev. B **55**, 9160 (1997).

²⁰R. Fehrenbacher and T. M. Rice, Phys. Rev. Lett. **22**, 3471 (1993).

²¹F. C. Zhang and T. M. Rice, Phys. Rev. B **37**, 3759 (1988).

²²G. Hilscher *et al.*, Physica C **22**, 330 (1994).